



ELSEVIER

Applied Surface Science 191 (2002) 344–351

applied  
surface science

www.elsevier.com/locate/apsusc

# Surface diffusion and electron stimulated desorption of chlorine from InP(1 1 0) and GaAs(1 1 0)

Marcus Jacka<sup>\*</sup>, Andy Kale

*Department of Physics, University of York, York YO10 5DD, UK*

Received 6 November 2001; accepted 27 March 2002

## Abstract

Using a parallel acquisition electron energy analyser (the HFA), the presence of sub-monolayer coverage of chlorine on in vacuo cleaved (1 1 0) surfaces of InP and GaAs has been observed. From the time evolution of the Auger features, together with sample absorption current images and residual gas analysis, it is apparent that both electron stimulated desorption and surface diffusion take place, and that these are influenced by the presence of two adsorption sites of differing strengths. In particular, the sample absorption current images provide a rapid means of measuring the spatial distribution of the chlorine thereby distinguishing the effects of desorption and diffusion. © 2002 Elsevier Science B.V. All rights reserved.

PACS: 79.20.L; 68.35.F

Keywords: Surface diffusion; Desorption; Auger; Parallel acquisition

## 1. Introduction

One effect of the continued miniaturisation of microelectronic circuits is the increased importance of adsorbed contaminants, which can appear unexpectedly by the action of surface diffusion. Common techniques for the chemical analysis of surfaces, such as Auger electron spectroscopy (AES), can fail to identify these adsorbates if the act of measuring removes the contaminant sufficiently rapidly, e.g., by electron stimulated desorption. This subject of surface changes due to electron beam radiation has been extensively reviewed by Pantano and Madey [1]. In the case of halogen compounds, which are routinely

used in semiconductor processing, a conventional Auger spectrometer will detect the sub-monolayer presence of these species if it is set to do so, but might be of little use without a priori knowledge. This is due to the serial manner in which the energy spectrum of scattered electrons is obtained, so that each energy channel in the spectrum has a longer irradiation time associated with it than the previous one. In the present work this problem is overcome by collecting the whole spectrum in parallel, using a novel electron energy analyser, the hyperbolic field analyser (HFA) [2,3]. With this device, time-dependent effects leading to changes in peak size, shape and position can be measured.

In experimental studies of electron stimulated desorption the effect of surface diffusion is often either ignored or else inferred from a non-exponential decay of the adsorbate coverage (e.g., the desorption of Cl

<sup>\*</sup> Corresponding author. Tel.: +44-1904-432-232;  
fax: +44-1904-432-214.  
E-mail address: mj13@york.ac.uk (M. Jacka).

from Cu(1 1 1) [4]). Alternatively, such non-exponential behaviour has been ascribed to the presence of two adsorption sites of differing strength, such as for Cl on GaAs [5]. A difficulty arises because each of these scenarios can lead to very similar decay curves. On the theoretical side considerable work has been done on the problem of diffusion on surfaces of two adsorption sites [6,7]. This has led, e.g., to a good understanding of the effect of adsorbate coverage on surface diffusion. To our knowledge, little work has been done on the combined effects (i.e., concurrent desorption and surface diffusion in the presence of two adsorption sites) despite the fact that where the former exists, the latter is likely to also. One exception to this [7] involves thermal desorption and surface diffusion. In this case, the diffusion is treated at an atomic scale only, which is not directly relevant to practical problems in Auger microscopy.

The observable feature which distinguishes the effects of desorption and diffusion is the spatial distribution profile of the adsorbate across the irradiated area. A measure of this is useful as a means of linking the macroscopic experimental data (in this case the average Auger yield) with an understanding of the system based on microscopic interactions. To observe this we use a small spot-size electron beam, scanned over a well-defined area in order to control the irradiation intensity. This is contrary to the usual method, in which the surface is irradiated unevenly due to the profile of a large-area static beam, thereby disguising the effects of surface diffusion. We have noticed that the resulting diffusion modified coverage can be observed in the sample absorption current image. The great advantage of this technique is that it can be done rapidly and with sub-micron spatial resolution unlike, e.g., contact potential difference methods [8].

## 2. The parallel acquisition analyser and electron stimulated desorption

The HFA is an electrostatic deflection type electron energy analyser which has been described elsewhere [2,3]. Briefly, it can collect, in parallel, an energy spectrum within a range  $E_{\max}/E_{\min} \approx 34$ . Typically it is set to capture a spectrum from about 75 to 2600 eV but this can be changed by adjusting the analysing field strength. Electrons entering the analyser are

focused, according to their energy, onto a position sensitive detector. This consists of a microchannel plate, phosphor screen and 1024 channel linear photodiode array (Hamamatsu S3901-1024F). The phosphor screen and photodiode array are coupled by a fibre-optic plate. Each photodiode channel measures  $2500 \times 50 \mu\text{m}$ , giving a total effective length of 51 mm along which the energy spectrum is spread. The amplifier for the photodiode array is located outside the vacuum chamber. A 16-bit 100 ksamples/s DAC/ADC and National Instruments LabWindows written software handle the data acquisition and processing.

The strength of the HFA lies in its ability to measure spectra quickly, rather than being a high-resolution instrument, hence a spectrum can be acquired in under 50 ms. The quality depends on the electron probe current and the material being examined. For the copper 916 eV LMM peak the signal to noise ratio for a 5 keV incident beam is approximately  $3(It)^{1/2}$ , where  $I$  is the incident current in nanoamperes and  $t$  the acquisition time in seconds. Typically, one can obtain spectra with a signal to noise ratio of 10:1 in a few seconds or less with a probe current of nanoamperes. A spectrum obtained from InP is shown in Fig. 1(c).

Sections of 0.5 mm GaAs and InP wafer were mounted in a copper block and placed in the vacuum system. Once the pressure of less than  $10^{-9}$  mbar had been achieved the InP or GaAs samples were cleaved and measurements begun. All experiments were performed at room temperature. The samples were snapped perpendicular to the wafer face (1 0 0) and revealed a flat glassy surface, which could confidently be assigned (1 1 0). No ion bombardment was implemented.

Immediately after cleaving, AES shows only the (bulk) III, V components. After some minutes, however (during which the electron beam was not on the sample) the presence of chlorine (LMM peak at 176 eV) could be observed. In principle it would be possible to determine the surface diffusion behaviour from the rate at which the chlorine accrued on the surface, but the complicated geometry of the sample together with uncertainty as to the source of the adsorbate make it too difficult in this case.

A residual gas analyser (VG Gas Smart IQ<sup>+</sup>) was used to further identify the adsorbate. During desorption by the electron beam, masses 35, 36, 37 and 38

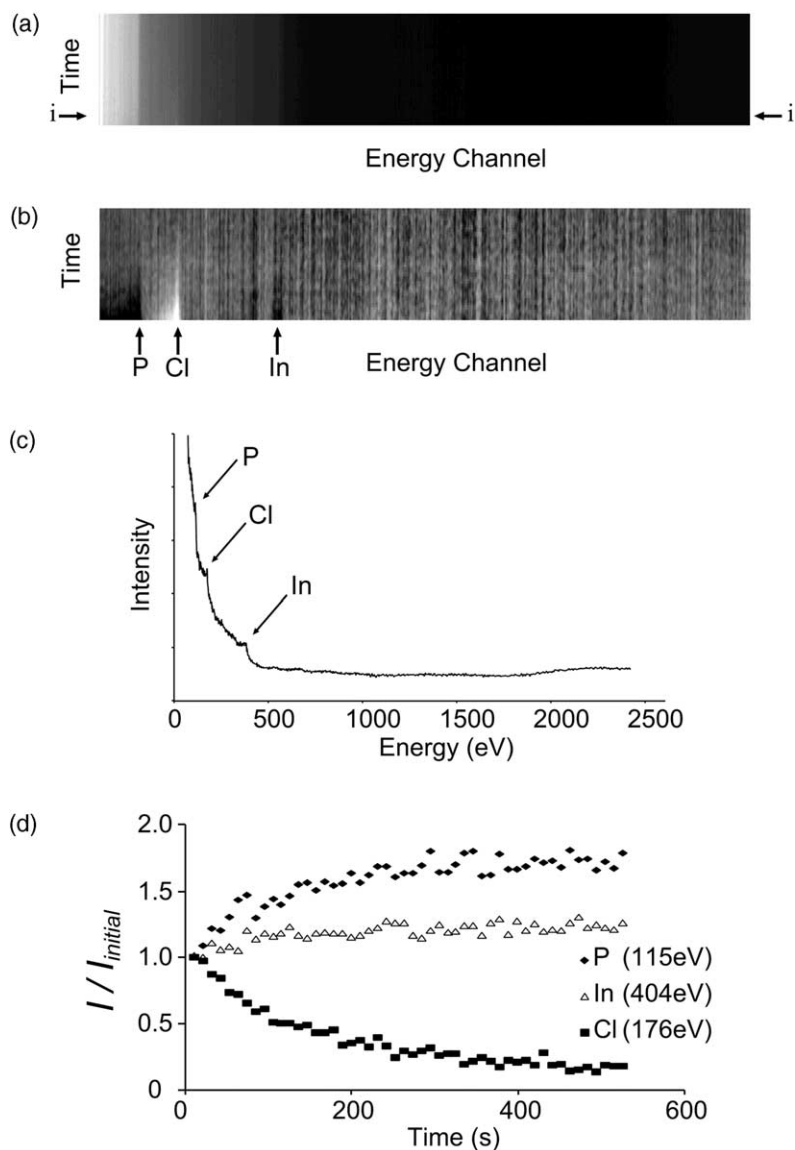


Fig. 1. InP(1 1 0)—(a) Time versus energy image made up of multiple spectra such as (c) (taken through i–i). To highlight the changing behaviour of the surface each energy channel can be divided by its final steady-state, giving the image (b). Cross-sections at constant energy show the evolution of individual Auger features (this time normalised by the initial value) (d).

were observed, although the partial pressure of each was less than  $10^{-13}$  mbar, at the limit of detectability. Taking into account cracking patterns and isotopes, the amount of each was consistent with the presence of HCl and Cl in the ratio 2:1. No other features associated with chlorine could be observed. It is supposed that the Cl originates from impurities in the copper

support, or else the silver paint between the sample and the mount. We are unsure about the mechanism producing HCl, or indeed whether it is present on the surface in that form.

An electrostatic single-lens field-emission electron gun was used for these experiments. The current was approximately 3 nA, and always at a fixed energy of

5 keV. The minimum beam spot size was approximately 200 nm although this could be made larger by defocusing. In general, however, the irradiation intensity was controlled by repeatedly and rapidly scanning the beam over a known area, ranging from  $3 \mu\text{m} \times 3 \mu\text{m}$  to  $80 \mu\text{m} \times 80 \mu\text{m}$ , giving intensities of between 0.5 and  $300 \text{ A m}^{-2}$ . Each spectrum was acquired in either 1, 5 or 10 s. Spectra were acquired sequentially until the Cl Auger signal had decayed appreciably. Sequences of spectra are displayed as images (Fig. 1(a) and (b)) showing the evolution of the surface. This is a somewhat unconventional way of displaying spectra but it allows all of the data from the parallel acquisition energy analyser to be displayed and highlights the time varying features.

Cross-sections through the image at constant energy show not only the decay of the chlorine peak but also the emergence of the bulk components (Fig. 1(d)). This gives us some insight into the location of the adsorbate. The change in thickness of adsorbate ( $\Delta C$ , in monolayers) can be determined from the attenuation of the Auger peaks ( $I$ ) of the underlying components according to

$$\Delta C = \frac{\lambda}{2.46} \ln \left( \frac{I_{\text{final}}}{I_{\text{initial}}} \right)$$

The mean free path for the escaping electrons can be approximated by  $\lambda = 0.2 \sqrt{E}$  [9] and the factor 2.46 comes from the  $24^\circ$  entrance angle of the analyser with respect to the sample surface. Taking Fig. 1(d) as an example, the P Auger electrons ( $E = 115 \text{ eV}$ ) are

attenuated by an adsorbate thickness of  $0.46 \pm 0.05$  monolayers, while for the In Auger electrons ( $E = 404 \text{ eV}$ ) the thickness is  $0.36 \pm 0.04$  monolayers. This suggests that the chlorine is located primarily on the P sites, which is consistent with the behaviour of Cl on GaAs derived from energy loss spectroscopy [5] and photoemission spectroscopy [10].

By the method of Chang [9], the average coverage can be determined from the measured intensity of all three Auger features ( $I_j$ ) together with knowledge of the bulk composition and relative sensitivity factors, using the expression

$$C = \frac{-\lambda}{2.46} \ln \left( 1 - \frac{\alpha_{\text{Cl}} I_{\text{Cl}}}{\sum_j \alpha_j I_j} \right)$$

The inverse relative sensitivity factors of the bulk components  $\alpha_j$  are taken as 1.05 and 2.22 for indium and phosphorous, 5.88 and 8.33 for gallium and arsenic, and  $\alpha_{\text{Cl}} = 1.0$  for chlorine [11].

Images were collected for each of the electron beam intensities, scanning over a fresh part of the surface each time. The decay signals for the chlorine Auger peak are independent of electron beam intensity when plotted on a coverage versus dose ( $\text{C m}^{-2}$ ) graph (Fig. 2). The curves show the best fits for three simple models described below.

The decay of the chlorine signal does not obey exponential behaviour (model A—time constant  $3.75 \times 10^{-4} \text{ A}^{-1} \text{ m}^2 \text{ s}^{-1}$ ), implying that either the adsorbate–surface interaction is non-uniform or else

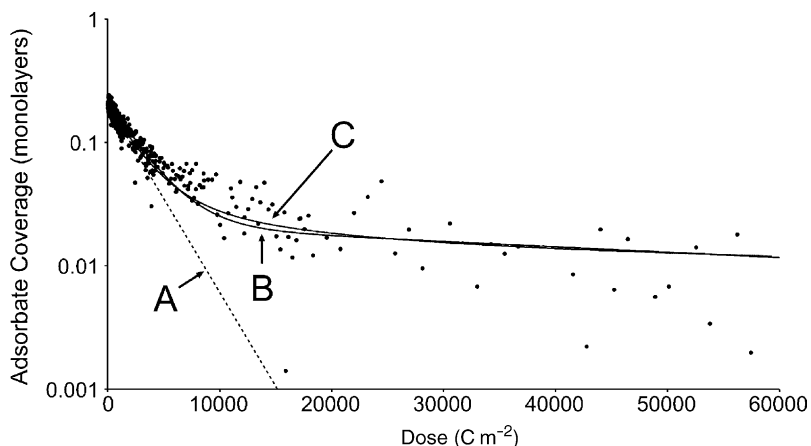


Fig. 2. Decay of Cl (LMM) signal. See text for details of models.

the adsorbate coverage is not solely controlled by the desorption process, but is moderated by surface diffusion. (There is a further possibility that this behaviour is due to a coverage-dependent energy of adsorption, however, in similar systems this effect is seen as a transition at one monolayer [5], whereas in this work the coverage is at all times sub-monolayer.)

If we suppose (in the manner of Troost et al. [5]), the existence of two adsorption sites, and no exchange of adsorbate between them, the decay would take the form of the sum of two exponential curves (model B—second time constant  $1.0 \times 10^{-5} \text{ A}^{-1} \text{ m}^2 \text{ s}^{-1}$ ), with the initial population of the sites being in the ratio nearly 10:1 (in favour of Cl–P). We will show later that this cannot be the sole mechanism.

Alternatively, we might assume that the adsorption is not site-specific and apply Fick's law to model the effect of surface diffusion. Solving this numerically using a relative difference equation is the most straightforward method and gives the flexibility to simulate different experimental conditions. A  $20 \times 20$  array is sufficient to model one-quarter of the irradiated region (the remaining three-quarters being mirror images of this).

For the region not under electron beam bombardment, the change in local adsorbate coverage ( $\Delta C_{x,y}$ ) after each time step is determined from the average of the gradients in both the  $x$  and  $y$  directions, i.e.

$$\Delta C_{x,y} = -\frac{D\Delta t}{4(\Delta x)^2}(C_{x-1} + C_{x+1} + C_{y-1} + C_{y+1})$$

where  $D$  represents the diffusion coefficient,  $\Delta t$  the size of the time step used and  $\Delta x$  the physical size of an array point in the model.

For the area being irradiated by the electron beam, an additional term  $\Delta C'_{x,y}$ , proportional to the amount of adsorbate present is removed, to simulate the electron stimulated desorption

$$\Delta C'_{x,y} = -\left(\frac{kJ\Delta t}{A}\right)C_{x,y}$$

Here,  $k$  is the desorption parameter,  $J$  the sample absorption current and  $A$  the area under illumination.

The decay curve (C) shows the average of the local coverage. This best fit has a diffusion coefficient of  $D = (7.0 \pm 1.4) \times 10^{-14} \text{ m}^2 \text{ s}^{-1}$ . The similarity between the models B and C is remarkable and they

cannot be distinguished on the basis of the experimental AES data. Further information is, however, available in the form of the coverage profile across the irradiated area. In the absence of surface diffusion this is of course flat-bottomed, whilst the values of  $C_{x,y}$  give the model distribution when diffusion is included. We next describe a method of measuring the coverage distribution in order to attempt to distinguish these possibilities.

### 3. Analysis of sample absorption current images—surface diffusion

Measurements of the diffusion modified coverage profile benefit from the use of the finely focussed electron beam, which, by scanning, can uniformly irradiate a well-defined area. It allows us to measure the diffusion across the border between the irradiated and non-irradiated regions. In contrast, others have used static broad and ill-defined electron beams [1,4], or for laser-induced thermal desorption, beams with a near-Gaussian profile [12].

The measure of changes in coverage comes from the observation that the sample absorption current decreases along with the decay of the chlorine Auger signal. (Since the sample current can be measured much more quickly than the Auger signal, sample current images can be obtained with very little desorption during the measurement.) The reverse effect (a signal increase) was apparent in the secondary electron yield, but to a much less degree, suggesting that the origin of this behaviour can be attributed primarily to a change in the backscattered electron yield. At lower incident energy (100 eV) Troost et al. [5] observed the opposite effect, i.e., a decrease in the backscattering coefficient when Cl was removed from a GaAs surface. This suggests a highly sensitive contrast mechanism which could be further developed.

This observation might also provide the explanation for the common phenomenon of patches appearing in secondary electron images in UHV microscopy, in regions which have been exposed to the electron beam, i.e., that the patches are caused by the removal of an adsorbate. At higher pressure similar effects can be explained by the cracking of hydrocarbons on the surface [13] but in UHV conditions this is implausible,

and there is no evidence for this in the carbon Auger signal. Dissociation of the surface due to the thermal effects of the electron beam could also contribute to the contrast. The arguments against this being significant are, firstly, that the thermal induced dissociation leads to an indium-rich surface [14], whereas our Auger analysis shows an increase in the phosphorous signal after exposure. Secondly, the desorption process and absorption current image profile are unaffected by moderate defocusing of the electron beam, which would significantly reduce local heating effects.

If the adsorbate is in the form of HCl, then a further complication is the possibility of the electron irradiation enhancing the etch rate of the substrate [15], however, this is again unlikely to be significant at room temperature.

In using the sample absorption current as a measure of the adsorbate coverage it is assumed that a linear relationship exists between the two. This is reasonable, particularly bearing in mind that the initial coverage is sub-monolayer. In this case the linear relationship between coverage of the constituents of

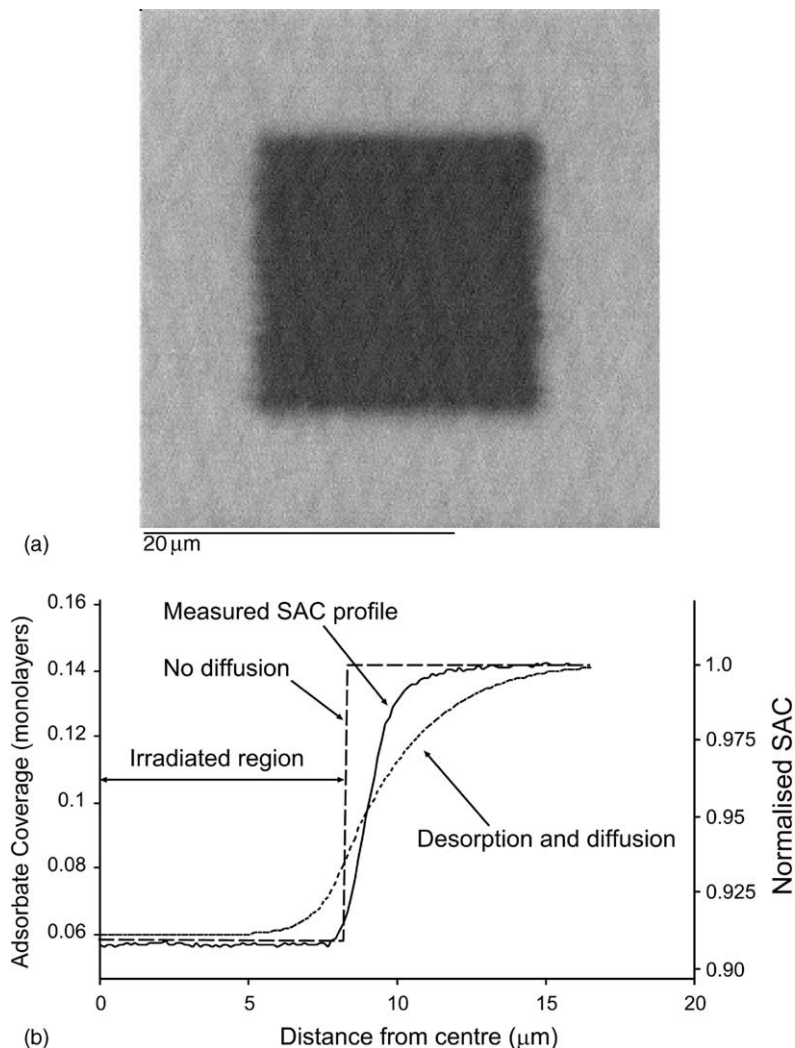


Fig. 3. (a) Sample absorption current image showing effect of electron beam radiation ( $8.5 \times 10^3 \text{ C m}^{-2}$  in the inner dark region) on InP. (b) Coverage profile across boundary of irradiated region. The electron beam spot size is  $\sim 0.2 \mu\text{m}$ . See text for model fits.

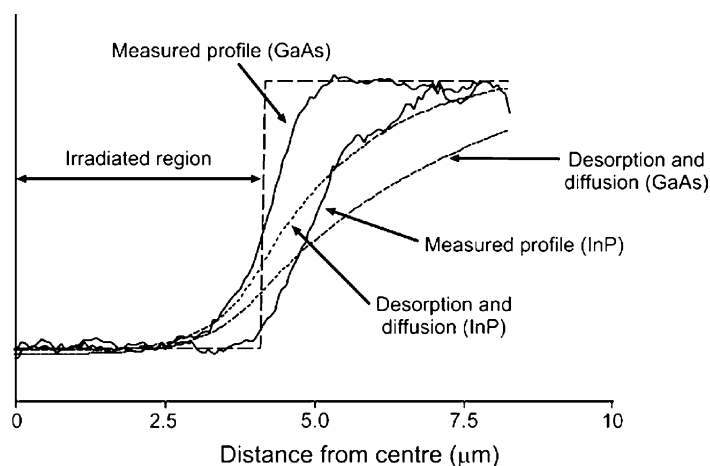


Fig. 4. Comparison of coverage profiles for InP and GaAs (dose in central irradiated region  $\sim 1.8 \times 10^4 \text{ C m}^{-2}$ ).

homogeneous compounds and backscattering coefficient (and therefore sample absorption current) [16] can be invoked.

Fig. 3(a) shows a typical sample absorption current image. The dark inner region is the area irradiated whilst the desorption was being measured. The magnification was then reduced by a factor of 2 and the scan slowed down to produce the final image. The coverage profile across the boundary between the irradiated and non-irradiated regions (Fig. 3(b)) is very much broader than the electron beam spot size, demonstrating that surface diffusion is in fact taking place. Also shown are the profiles predicted by the models fitted to the Auger Cl decay signal. Clearly, neither is satisfactory, suggesting that both effects are taking place.

Since the experimental data lies between the predictions of the two models, the models provide some measure of the desorption and diffusion parameters. The dominant desorption constant is similar for each model  $(3.75 \pm 0.3) \times 10^{-4} \text{ A}^{-1} \text{ m}^2 \text{ s}^{-1}$ , and the surface diffusion is less than  $(7.0 \pm 1.4) \times 10^{-14} \text{ m}^2 \text{ s}^{-1}$ . There is considerable difficulty in further quantifying the individual roles of the desorption and surface diffusion. The models such as those developed by Chvoj et al. [6] for diffusion in the presence of two adsorption sites could be modified relatively easily to include desorption, but the parameter space is too large to find a unique solution fitting the present experimental data. This would involve a full description

of the coverage dependence of the surface diffusion parameter.

#### 4. Comparison between InP(1 1 0) and GaAs(1 1 0)

The experiments were repeated using a cleaved GaAs(1 1 0) sample, and broadly the results were similar. Fig. 4 shows the diffusion modified coverage profile across the scanned region for both InP and GaAs after similar electron beam exposure, in each case with the model fit to the Cl Auger decay curve. It is apparent that for GaAs the desorption parameter is greater and the surface diffusion is less pronounced.

#### 5. Conclusion

The results presented demonstrate the adsorption of Cl to GaAs and InP(1 1 0) on two sites of differing bond strength, of which the Cl–As and Cl–P are the stronger. Measurements of the desorption parameters are not possible purely from the rate of desorption because of the moderating effect of surface diffusion. The use of sample current absorption images provides a remarkably sensitive measure of changes in adsorbate coverage in the sub-monolayer regime, and warrants further investigation as to its general applicability to rapid measurements of surface diffusion.

## Acknowledgements

The authors wish to acknowledge the interest, and useful discussions held with Prof. Martin Prutton. AK thanks Shimadzu Research Laboratories (Europe) Ltd. and the Engineering and Physical Sciences Research Council for the provision of a CASE studentship.

## References

- [1] C.G. Pantano, T.E. Madey, *Appl. Surf. Sci.* 7 (1981) 115.
- [2] M. Jacka, *J. Electron Spectrosc.* 114 (2001) 277.
- [3] M. Jacka, M. Kirk, M.M. El Gomati, M. Prutton, *Rev. Sci. Inst.* 70 (1999) 2282.
- [4] W.K. Walter, D.E. Manolopoulos, R.G. Jones, *Surf. Sci.* 348 (1996) 115.
- [5] D. Troost, H.J. Clemens, L. Koenders, W. Mönch, *Surf. Sci.* 286 (1993) 97.
- [6] Z. Chvoj, H. Conrad, V. Cháb, M. Ondrejcek, A.M. Bradshaw, *Surf. Sci.* 329 (1995) 121.
- [7] V.P. Zhdanov, P.R. Norton, *Surf. Sci.* 350 (1995) 271.
- [8] A.G. Naumovets, Y.S. Vedula, *Surf. Sci. Rep.* 4 (1985) 365.
- [9] C.C. Chang, *Surf. Sci.* 48 (1975) 9.
- [10] G. Margaritondo, J.E. Rowe, C.M. Bertoni, C. Calandra, F. Manghi, *Phys. Rev. B* 20 (1979) 1538.
- [11] T. Sekine, et al., *Handbook of Auger Electron Spectroscopy*, JEOL, 1982.
- [12] E.D. Westre, D.E. Brown, J. Kutzner, S.M. George, *Surf. Sci.* 294 (1993) 185.
- [13] C.A. Kondoleon, *J. Vac. Sci. Technol. A* 18 (2000) 2699.
- [14] M. Gajdardziskajosifovska, M.H. Malay, D.J. Smith, *Surf. Sci.* 340 (1–2) (1995) 141.
- [15] K. Akita, Y. Sugimoto, H. Kawanishi, *Semiconduct. Sci.* 6 (9) (1991) 934.
- [16] R. Herrmann, L. Reimer, *Scanning* 6 (1984) 20.